

MARCKS regulates membrane targeting of Rab10 vesicles to promote axon development

Xiao-Hui Xu^{1,2,*}, Cai-Yun Deng^{1,*}, Yang Liu¹, Miao He¹, Jian Peng^{1,3}, Tong Wang¹, Lei Yuan¹, Zhi-Sheng Zheng¹, Perry J Blackshear⁴, Zhen-Ge Luo¹

¹Institute of Neuroscience and State Key Laboratory of Neuroscience, Shanghai Institutes for Biological Sciences, Chinese Academy of Sciences, Shanghai 200031, China; ²School of Life Sciences, Shanghai University, Shanghai 200444, China; ³School of Life Science and Technology, ShanghaiTech University, Shanghai 200031, China; ⁴Laboratory of Signal Transduction, National Institute of Environmental Health Sciences, Research Triangle Park, NC 27709, USA

Axon development requires membrane addition from the intracellular supply, which has been shown to be mediated by Rab10-positive plasmalemmal precursor vesicles (PPVs). However, the molecular mechanisms underlying the membrane trafficking processes of PPVs remain unclear. Here, we show that myristoylated alanine-rich C-kinase substrate (MARCKS) mediates membrane targeting of Rab10-positive PPVs, and this regulation is critical for axon development. We found that the GTP-locked active form of Rab10 binds to membrane-associated MARCKS, whose affinity depends on the phosphorylation status of the MARCKS effector domain. Either genetic silencing of MARCKS or disruption of its interaction with Rab10 inhibited axon growth of cortical neurons, impaired docking and fusion of Rab10 vesicles with the plasma membrane, and consequently caused a loss of membrane insertion of axonal receptors responsive to extracellular axon growth factors. Thus, this study has identified a novel function of MARCKS in mediating membrane targeting of PPVs during axon development.

Keywords: MARCKS; Rab10; plasmalemmal precursor vesicles; axon growth

Cell Research (2014) 24:576–594. doi:10.1038/cr.2014.33; published online 25 March 2014

Introduction

Myristoylated alanine-rich C-kinase substrate (MARCKS) was first identified as a prominent substrate for protein kinase C (PKC) [1, 2]. It is associated with plasma membrane (PM) through its N-terminal myristoylation site and the basic effector domain (ED), and phosphorylation of MARCKS by PKC abrogates its membrane tethering, leading to its translocation into the cytosol [3–6]. In addition, MARCKS binds to actin [7], serves to sequester phosphatidylinositol 4,5-bisphosphate [PI(4,5)P₂] at plasmalemmal rafts [8], and regulates membrane ruffling and cell spreading [9]. MARCKS is highly enriched in the brain, particularly at early developmental stages [10–13]. Genetic studies show that

MARCKS plays an important role in the development of the central nervous system, including neurulation, fusion of the cerebral hemispheres, formation of the forebrain commissures, and lamination of the cortex and retina [14]. Moreover, MARCKS is critical for neurite initiation, dendritic branching, spine maintenance [15–17], growth cone adhesion and path finding [18], and neuronal migration [19, 20]. However, the direct linkage between the biochemical properties of MARCKS and its cellular functions has not been well established.

In eukaryotic cells, the Rab family members of small GTPases are involved in various membrane trafficking events, including formation of transport vesicles, trafficking along cytoskeletal tracks, and docking and fusion with the acceptor membrane [21, 22]. Among more than 60 Rabs, Rab8 and Rab10 have been shown to mediate directed membrane insertion during axon development [23, 24]. Indeed, Rab10 is associated with plasmalemmal precursor vesicles (PPVs) that are required for polarized membrane insertion during axon development [24].

Here, we have identified MARCKS as a component of

*These two authors contributed equally to this work.

Correspondence: Zhen-Ge Luo

E-mail: zglo@ion.ac.cn

Received 5 August 2013; revised 31 December 2013; accepted 25 February 2014; published online 25 March 2014

docking and fusion machinery for Rab10-positive PPVs. In addition, we have shown that the MARCKS-Rab10 system is critical for membrane insertion of axonal surface proteins and axonal elongation.

Results

Rab10 binds to MARCKS through effector domain

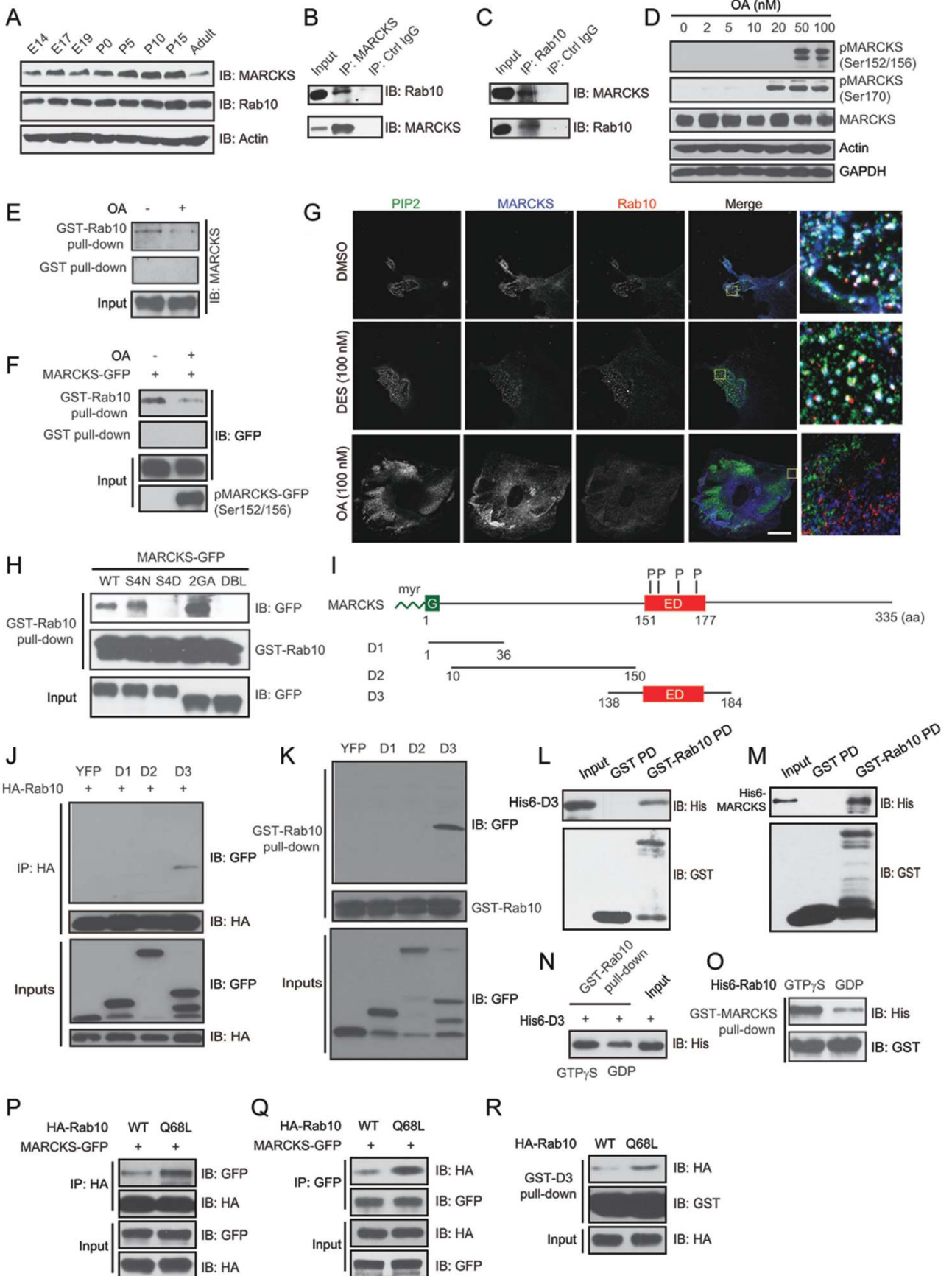
To gain insights into the mechanisms of Rab10 action in membrane insertion, we identified binding proteins by affinity purification from P0 rat brain lysates using glutathione S-transferase (GST)-Rab10, followed by analysis with liquid chromatography with tandem mass spectrometry (LC-MS). In addition to several known Rab10-binding partners, such as AS160, a GTPase-activating protein (GAP) for Rab10 [25], or Myosin V [26, 27], we also identified MARCKS as one of the interesting hits. Indeed, both MARCKS and Rab10 were expressed in the rat brain at early or late developmental stages (Figure 1A). Interestingly, in the neocortex of rats at E18.5, MARCKS and Rab10 were particularly enriched in the axonal tracts that were marked by axonal marker Smi312 (Supplementary information, Figure S1A). In rat brain homogenates, these two proteins co-immunoprecipitated with each other (Figure 1B and 1C). Given that phosphorylation of four serines within the ED is essential for the function and localization of MARCKS [28, 29], we determined whether the phosphorylation state of MARCKS influenced its interaction with Rab10. For this purpose, cultured cortical neurons were treated with okadaic acid (OA), a specific inhibitor for protein phosphatases (PP) 1 and 2A, which prevented dephosphorylation of

MARCKS [30]. OA treatment induced accumulation of phosphorylated endogenous (Figure 1D) or exogenous MARCKS (Figure 1F). Notably, OA treatment decreased the amount of MARCKS pulled down by GST-Rab10 (Figure 1E and 1F), suggesting that phosphorylation of MARCKS negatively regulates its interaction with Rab10.

Next, we determined subcellular localization of MARCKS and Rab10, and found that both proteins were largely colocalized in membrane microdomains of cell protrusions that were enriched with PI(4,5)P2 (Figure 1G). Notably, treatment with OA, but not the PP2A activator D-erythro-Sphingosine (DES) [31], caused dispersion of MARCKS and Rab10 signals (Figure 1G), in line with the notion that MARCKS phosphorylation negatively regulates its membrane association and interaction with Rab10. To further determine which state of MARCKS binds to Rab10, we took advantage of several mutated forms of MARCKS: S4N, a constitutively non-phosphorylatable form in which four serines in the ED were replaced by asparagines; S4D, a phosphomimetic form in which four serines were replaced by aspartic acid; G2A, a nonmyristoylatable form in which glycine at position 2 was replaced by alanine; and DBL, a nonmyristoylatable, pseudo-phosphorylated form with double mutations at S4D and G2A [32, 33]. Interestingly, we found that GST-Rab10 pulled down wild type (WT), S4N, or G2A, but not S4D or DBL (Figure 1H). This result suggests that Rab10 binds to unphosphorylated MARCKS in a myristoylation-independent manner.

To map the MARCKS domain that mediates the interaction with Rab10, we generated three constructs that

Figure 1 Rab10 interacts with MARCKS. **(A)** Expression of Rab10 and MARCKS in the rat brain at different developmental stages. **(B, C)** Co-immunoprecipitation (co-IP) of Rab10 and MARCKS in homogenates of P0 rat brains. **(D)** Cortical neurons at DIV2 were treated with different concentrations of OA for 6 h. Cell lysates were subjected to immunoblotting (IB) with antibodies against MARCKS or phosphorylated MARCKS (pMARCKS), with GAPDH or actin as loading control. **(E)** Cell lysates from cultured cortical neurons treated with OA (100 nM, 6 h) or vehicle at DIV2 were subjected to pull-down with glutathione-sepharose beads coupled to GST-Rab10 or GST, followed by IB with MARCKS antibody. **(F)** HEK293 cells transfected with GFP-MARCKS were treated with OA (100 nM) or vehicle for 6 h. Cell lysates were subjected to pull-down with glutathione-sepharose beads coupled to GST-Rab10 or GST. Bound proteins were subjected to IB with the indicated antibodies. **(G)** Rat fibroblasts were treated with DMSO, DES (100 nM), or OA (100 nM) for 2 h, followed by fixation (4% PFA) and penetration with 0.2% saponin, and then stained with antibodies against PIP2 (green), MARCKS (blue), and Rab10 (red). Scale bar, 15 μ m. **(H)** Cell lysates from HEK293 cells transfected with various MARCKS constructs tagged with GFP at the C-terminus were subjected to pull-down with glutathione-sepharose beads coupled to GST-Rab10 (5 μ g), followed by IB with GFP or GST antibody. **(I)** Schematic structure of MARCKS full-length protein or domains. ED, effector domain. **(J)** Cell lysates from HEK293 cells co-transfected with HA-Rab10 and YFP-tagged MARCKS domains were subjected to IP with anti-HA antibody, and then IB with anti-HA or GFP antibody. **(K)** GST-Rab10 pull-down of MARCKS domains expressed in HEK293 cells. **(L, M)** GST-Rab10 immobilized on glutathione-sepharose beads were incubated with purified His6-MARCKS or His6-D3. Bound proteins were subject to IB with the indicated antibodies. **(N)** Purified GST-Rab10 (2 μ g) preloaded with GTP γ S or GDP was used to pull down His6-D3. **(O)** Purified GST-MARCKS was used to pull down His6-Rab10 preloaded with GTP γ S or GDP. **(P, Q)** Lysates of HEK293 cells transfected with the indicated constructs were subject to IP and IB with the indicated antibodies. **(R)** GST-D3 pull-down of Rab10 (WT or Q68L form) expressed in HEK293 cells.



were fused with YFP at the C-terminus: D1 (1-36 aa), which contains the N-terminal myristoylation site, D2 (10-150 aa), and D3 (138-184 aa), which covers the ED region (Figure 1I). We found that in either co-immunoprecipitation (co-IP) (Figure 1J) or pull-down (Figure 1K) assays, Rab10 was associated with D3. The interaction between Rab10 and MARCKS is direct, because purified GST-Rab10, but not GST alone, could pull down purified hexahistidine (His6)-tagged D3 or full-length MARCKS (Figure 1L and 1M). Importantly, His6-D3, or GST-MARCKS, preferentially interacted with Rab10 preloaded with GTP γ S (a nonhydrolyzable GTP analog), compared to that preloaded with GDP (Figure 1N and 1O). In addition, co-IP and pull-down assays showed that MARCKS or D3 preferentially interacted with Rab10^{Q68L}, the GTP-locked active form of Rab10, rather than the WT (Figure 1P-1R). Thus, MARCKS might be an effector of Rab10.

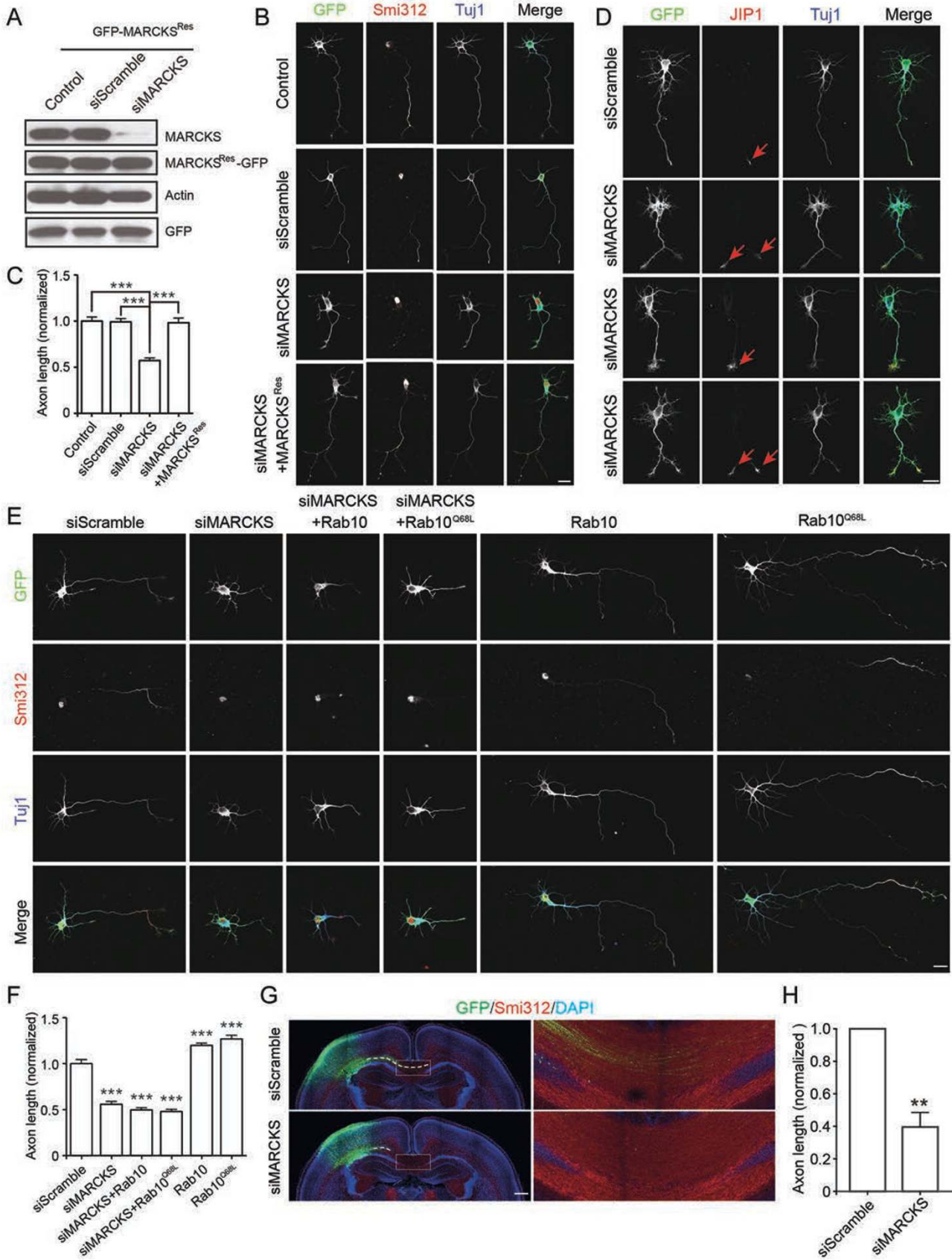
MARCKS interaction with Rab10 is important for axon development

Having known the interaction between MARCKS and Rab10 (Figure 1) and the enrichment of these two proteins in axonal tracts (Supplementary information, Figure S1A), we next investigated the role of MARCKS-Rab10 system in axon development. Indeed, both MARCKS and Rab10 were enriched in distal regions of axons (Supplementary information, Figure S1B-S1E), where membrane insertion happens during axon development [24, 34, 35]. We found that downregulation of MARCKS by transfection with a construct encoding small interfering RNA (siRNA) against MARCKS (siMARCKS) (Figure 2A) resulted in a marked decrease in total axon length, compared to vehicle control or scrambled siRNA in cultured cortical neurons (Figure 2B and 2C). The identity of nascent axons was determined by positive staining

with axonal marker Smi312 (Figure 2B), or c-Jun-amino-terminal kinase-interacting protein 1 (JIP1) (Figure 2D), a scaffold protein specifically localized in axon terminals and essential for axon development in cultured cortical neurons [36]. The impairment in axon growth was significantly prevented by co-expression of MARCKS^{Res}, the siRNA-resistant form of MARCKS (Figure 2A-2C), thus excluding potential off-target effects of siRNA. The axon development defect caused by siMARCKS was not due to the effect on cell health or general impairment in neurite extension, as indicated by similar low percentage of apoptotic cells with condensed nuclei and number of minor neurites in both control and siMARCKS groups (Supplementary information, Figure S2A-S2C).

Recently, we have shown that Rab10 promotes axon development [24]. However, overexpression of Rab10 or its constitutive active form Q68L failed to promote axon growth in MARCKS-knockdown neurons (Figure 2E and 2F). Thus, MARCKS is essential for the role of Rab10 in promoting axon growth. In contrast to MARCKS downregulation, overexpression of either WT MARCKS or its S4N form, but not the S4D or DBL form, caused an increase in total axon length, as well as the number of axon branches (Supplementary information, Figure S3A-S3C). Thus, dephosphorylated MARCKS, which has been shown to be associated with the PM [32, 33], where it interacts with Rab10 (Figure 1), supports axon growth. Notably, overexpression of the G2A form of MARCKS, which failed to be myristoylated and still associated with Rab10, caused a decrease in axon length, and interestingly, a significant increase in neurite branches (Supplementary information, Figure S3A-S3C). It has been shown previously that G2A form of MARCKS exhibits only a partial reduction in the association with the PM [5] and causes mis-targeting of some polarity proteins, such as Par3, during cell positioning [19]. The association of

Figure 2 MARCKS is important for axon development. **(A)** Cortical neurons were transfected with pSUPER vector or pSUPER encoding siRNAs against MARCKS (siMARCKS) or scrambled sequence (siScramble) together with MARCKS^{Res}. Endogenous MARCKS and MARCKS^{Res} levels were analyzed by IB with antibody against MARCKS or GFP, respectively. Actin and vector-encoded GFP were probed as controls. **(B)** Isolated cortical neurons were transfected with EGFP, siScramble, or siMARCKS, either alone or together with MARCKS^{Res}. At DIV3, cultures were fixed and analyzed for axon length. Scale bar, 20 μ m. **(C)** Quantification of normalized axon length. Data are shown as mean \pm SEM. At least 80 neurons from three independent experiments were analyzed. *** P < 0.001, one-way ANOVA. **(D)** DIV3 cortical neurons transfected with siScramble or siMARCKS were stained with anti-JIP1 and Tuj1 antibodies. Note the specific localization of JIP1 in axonal tips (red arrows). Scale bar, 20 μ m. **(E)** Isolated cortical neurons were transfected with various plasmid combinations, and then stained with Smi312 and Tuj1 at DIV3. Scale bar, 20 μ m. **(F)** Quantification of normalized axon length. Data are shown as mean \pm SEM. At least 80 neurons from three independent experiments were analyzed. *** P < 0.001, one-way ANOVA. **(G, H)** P2 neocortical slices from rat embryos electroporated at E16.5 with plasmids encoding siScramble or siMARCKS, together with pCAG-EYFP, were analyzed for axon development. Smi312 was used to label axonal tracts. Enlarged areas indicate axon tracts coursing through the intermediate zone (IZ). The length of these axon bundles, as sketched by dashed lines which delineate the path of axonal tracts in the IZ, was quantified with the value from control group normalized as 1.0 **(H)**. Data are presented as mean \pm SEM. At least four animals in each group were analyzed. ** P < 0.01, Student's *t*-test. Scale bar, 500 μ m.



Rab10 with G2A-containing membrane regions may result in mis-targeting of Rab10-positive vesicles, leading to excessive neurite branching.

The role of MARCKS in axon growth was further determined *in vivo* by *in utero* electroporation of siMARCKS or control plasmid into cortical neural precursors of rats at E16.5. At P2, we measured the length of axon bundles traversing through the intermediate zone (IZ) toward the midline, and found that siMARCKS transfection caused a marked decrease in the length of these corpus callosum axons (Figure 2G and 2H). Thus, MARCKS plays an important role in axon growth.

Next, we determined the role of MARCKS-Rab10 interaction in axon growth. As shown in Figure 3A, overexpression of D3 prevented the association between MARCKS and Rab10. When transfected into cultured cortical neurons, D3 caused a marked reduction in total axon length, compared to vehicle control or D1 (Figure 3B-3D), without deleterious effects on cell health or minor neurite formation (Supplementary information, Figure S2A-S2C). Similar to siMARCKS, *in utero* electroporation of D3 also inhibited elongation of corpus callosum axons *in vivo* (Figure 3E and 3F). These results suggest that MARCKS-Rab10 interaction is required for Rab10's axon growth-promoting activity.

MARCKS mediates docking and fusion of Rab10 vesicles with the plasma membrane

How does MARCKS-Rab10 interaction affect axon growth? Given the membrane localization of dephosphorylated MARCKS and the interaction with Rab10 in particular membrane domains, we hypothesized that MARCKS might be a component of docking or fusion machinery for Rab10 vesicles. At first, we tested this possibility by examining the behavior of tdTomato-Rab10 (TD-Rab10) in the vicinity of the PM, using Total Internal Reflection Fluorescence Microscopy (TIRFM), which allows selective imaging of fluorescent signals within the close proximity (< 200 nm) of the coverslip, in nonpolarized fibroblasts, which have much larger soma areas. A complete fusion event is composed of the following consecutive steps: predocking period after initial immobilization with vesicles transiently on or off from the target sites; stable immobilization before fusion with vesicles stably anchored to the PM; and finally, fusion of vesicles followed by lateral diffusion of fluorescence signals (Figure 4A, see the bars for the changes of fluorescent intensity of Rab10 over time, and Supplementary information, Movie S1). We measured numbers of fusion events, which were composed of complete cycles of docking, fusion and diffusion (Supplementary information, Figure S4B), but not those only with transient kiss-

and-run patterns (Supplementary information, Figure S4C), during 5 min observation periods. We found that in cells transfected with siMARCKS, the number of fusion events was markedly decreased (Figure 4B and Supplementary information, Movie S2), and this decrease could be rescued by expression of MARCKS^{Res} (Figure 4B). Occasionally, Rab10 TIRF signals in siMARCKS cells exhibited highly dynamic trajectory on the membrane plane, indicating unstable association of Rab10 vesicles with the PM target domains (Supplementary information, Movie S3). By contrast, upregulation of MARCKS by overexpressing WT MARCKS increased the number of fusion events (Figure 4C). Notably, whereas overexpression of D3 reduced the number of fusion events (Figure 4C), it usually caused persistence of tubule-like structures in the cell cortex (Supplementary information, Figure S4A, S4D, S4E and Movie S4), and indeed, the majority (~80%) of D3-transfected cells exhibited tubule-like structures, compared to a much lower percentage of tubule-bearing cells in control or D2-transfected cells (Supplementary information, Figure S4F). These phenomena could be caused by the failure in the fusion of docked vesicles. The D3-induced Rab10 tubules were much different from those caused by downregulation of Myosin Vb (MYO5B) (Supplementary information, Figure S4E), which has been shown recently to control fission of Rab10 carriers from the trans-Golgi network (TGN) [27], because MYO5B knockdown-induced tubules were distributed in peri-nuclear regions and derived from TGN and MARCKS D3-induced Rab10 tubules were associated with the PM (Supplementary information, Figure S4D and S4E). Actually, D3 itself can associate with the PM (Supplementary information, Figure S5A and S5B), and may still mediate docking of Rab10 vesicles without successful fusion. In line with this notion, although epifluorescence (epi-F) signals of TD-Rab10 were not changed in siMARCKS- or D3-transfected cells, the TIRF signals were decreased in siMARCKS cells and increased in D3 cells (Figure 4D). Thus, MARCKS mediates docking of Rab10 vesicles, most likely through D3. We also analyzed the effects of mutations in myristoylation or phosphorylation sites of MARCKS on the fusion behavior of Rab10 vesicles, and found that expression of S4N increased the frequency of fusion, S4D or DBL exhibited an opposite effect, and G2A showed a mild but not significant effect (Figure 4E). These results suggest that MARCKS plays an important role in the docking of Rab10-positive vesicles. In support of the above conclusion, Fluorescence Resonance Energy Transfer (FRET) analysis showed that Rab10 interacted with MARCKS in certain patches of the PM (Supplementary information, Figure S6A, S6C and

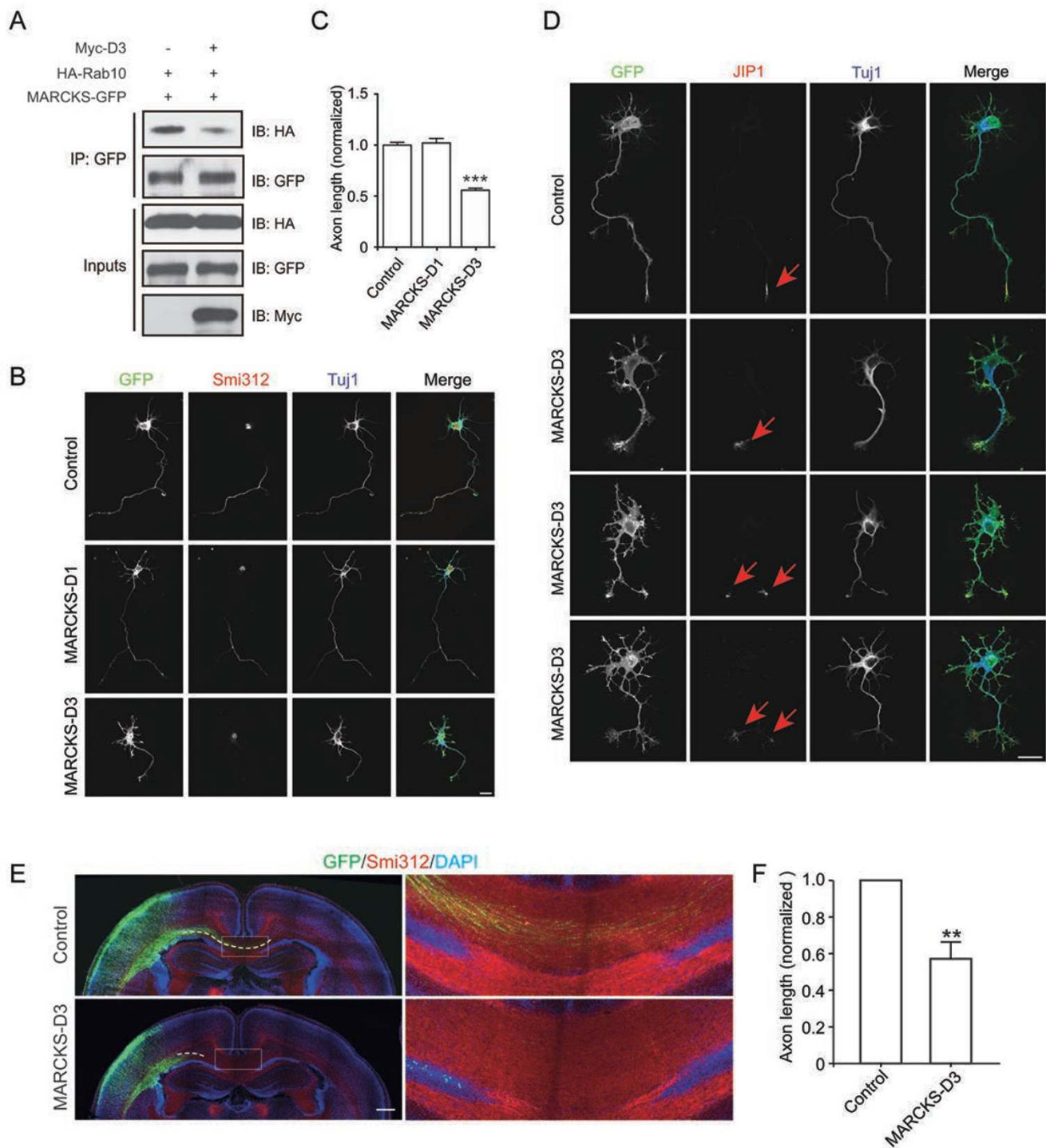


Figure 3 MARCKS interaction with Rab10 is important for axon development. **(A)** The association between Rab10 and MARCKS was blocked by D3 expressed in HEK293 cells. **(B, C)** Representative images of DIV3 cortical neurons transfected with vehicle plasmid or that encoding MARCKS D1 or D3 fragment **(B)** and quantification of the axon length **(C)**. Data are shown as mean \pm SEM. At least 100 neurons from three independent experiments were analyzed. *** $P < 0.001$, one-way ANOVA. Scale bar, 20 μ m. **(D)** DIV3 cortical neurons transfected with vehicle plasmid or that encoding D3 fragment were stained with anti-JIP1 and Tuj1 antibodies. Arrows indicate JIP1 signals in axonal tips. Scale bar, 20 μ m. **(E, F)** Representative images of P2 neocortical slices from rat embryos, which were electroporated at E16.5 with vehicle or D3 plasmids, together with pCAG-EYFP **(E)** and the quantification of corpus callosum axon length **(F)**. Data are presented as mean \pm SEM. At least five animals in each group were analyzed. ** $P < 0.01$, Student's *t*-test. Scale bar, 500 μ m.

S6D). In contrast, no FRET signals were observed between MARCKS and Rab11, a member of Rab family of small GTPases involved in vesicle recycling and neurite growth [37] (Supplementary information, Figure S6B-S6D). In addition, the fusion events of Rab11 vesicles were not changed in siMARCKS- or D3-transfected cells (Supplementary information, Figure S6E), suggesting the specificity of MARCKS in Rab10 membrane targeting. The spatial relationship between Rab10 and MARCKS was also determined by transmission electronic microscopy (TEM). We found that in the P0 rat brain sections covering the regions of callosal commissure, most immunogold particles (12 nm) for Rab10 (~60%) were found in vesicles that were in the vicinity of the PM sites labeled by 18 nm particles for MARCKS (Figure 4F and 4G). The size of these vesicles ranged between 150 and 200 nm in diameter, similar to that of PPVs [24, 35].

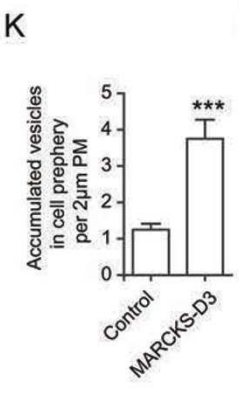
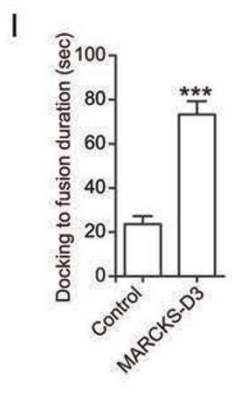
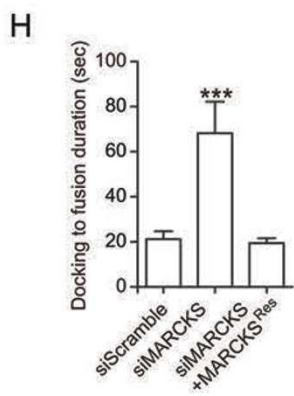
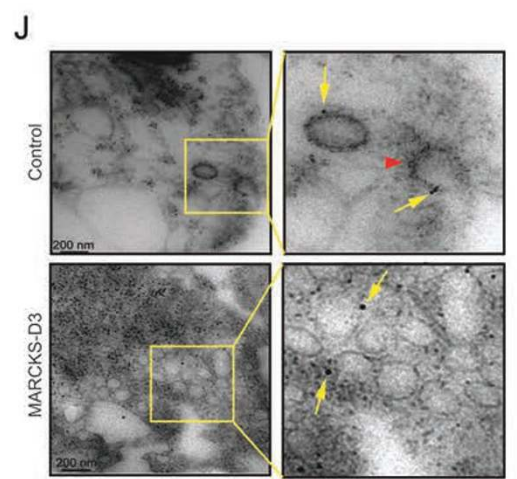
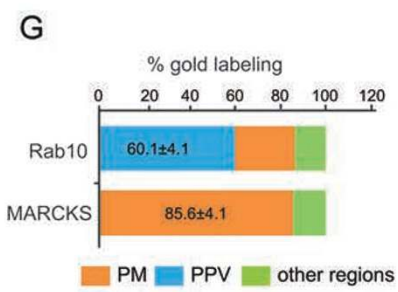
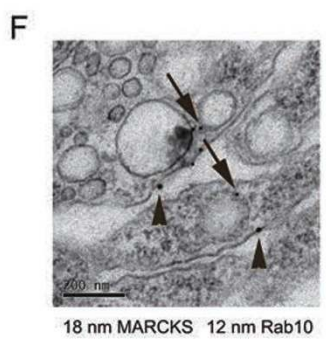
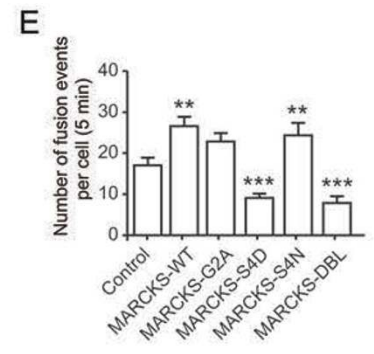
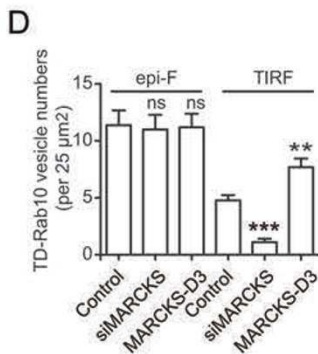
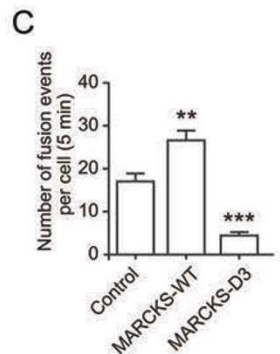
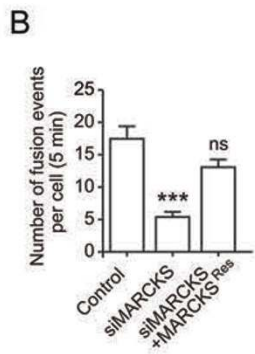
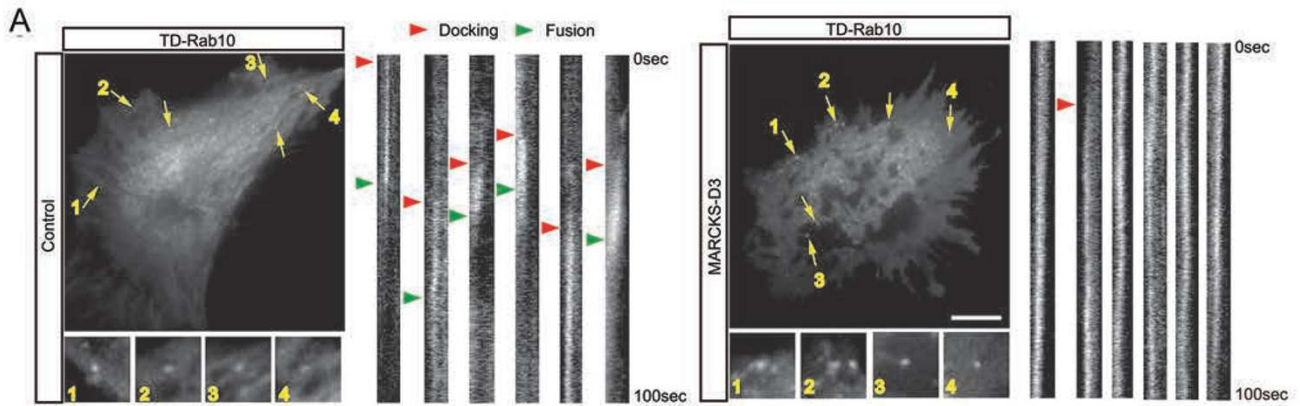
To further determine the dynamic process for the membrane fusion of Rab10 vesicles, we analyzed the durations for each fusion event, which reflected vesicle fusion efficiency (Figure 4A and Supplementary information, Figure S4B). We noted that the pause duration between stable docking and fusion with the PM was markedly increased in siMARCKS- or D3-transfected cells (Figure 4A, 4H, 4I and Supplementary information, Figure S4B), and the defect caused by siMARCKS could be rescued by MARCKS^{Res} (Figure 4H). This result indicates that MARCKS is also important for the fusion of Rab10-positive PPVs. Membrane fusion of Rab10 vesicles was further determined by TEM analy-

sis for immunogold-labeled vesicles localized at or near the PM. As shown in Figure 4J, omega-shaped Rab10-positive structures on the PM, which represent either membrane fusion or endocytosis, were often seen in control cells, whereas in D3-transfected cells, these structures were seldom observed. Notably, numerous Rab10 vesicles accumulated in the periphery of D3 cells (Figure 4J and 4K). The observed changes in the pattern of Rab10 vesicles may not be due to impairment in the behavior of endosomes, because expression of D3 had no effect on the endocytosis of transferrin ligand, which exhibited distinct localization with Rab10 (Supplementary information, Figure S7A and S7B). These results can be interpreted as that D3 domain of MARCKS is sufficient to mediate membrane docking, but not fusion, of Rab10 vesicles and that overexpression of D3 abrogates Rab10 interaction with endogenous MARCKS, which may be associated with fusion machinery through other domains.

MARCKS regulates membrane insertion of PPVs in cultured cortical neurons

Next, we determined the role of MARCKS in membrane insertion of PPVs in neurons. As shown in our previous study, we have used BODIPY-ceramide (BODIPY FL C₅-ceramide), a fluorescent sphingomyelin and glucosylceramide precursor [38], to label PPVs in cultured cortical neurons [24]. After labeling, uptake and extensive washes (see Figure 5A), we followed the dynamic changes for the fluorescence intensity of BODIPY-red signals, which were used to monitor membrane insertion

Figure 4 MARCKS interaction with Rab10 is important for vesicle docking and fusion. **(A)** TIRFM analysis for the fusion pattern of individual TD-Rab10 vesicles in rat fibroblasts transfected with the indicated plasmids. Individual fusion events are numbered and indicated by yellow arrows. Right bars are the changes of fluorescent intensity of TD-Rab10 vesicles (arrows in left image) over time. Note the persistence of Rab10 signals associated with the PM in D3 cells during the 100 s observation period. Docking and fusion are indicated with red arrowheads and green arrowheads, respectively. Scale bar, 10 μ m. **(B, C)** Quantification of average numbers of fusion events with complete cycles of docking and fusion during 5 min observation time in each cell transfected with the indicated plasmids. Data are presented as mean \pm SEM. At least eight cells in each group were analyzed. ** $P < 0.01$, *** $P < 0.001$, n.s., not significant, Student's *t*-test. **(D)** Average number of TD-Rab10 vesicles per 25 μ m² in fixed cells. Epifluorescence (epi-F) and TIRF signals represent total and PM-associated Rab10, respectively. Data are presented as mean \pm SEM. At least eight cells in each group were analyzed. ** $P < 0.01$, *** $P < 0.001$, n.s., not significant, one-way ANOVA. **(E)** Quantification of average numbers of fusion events in the indicated groups. Data are presented as mean \pm SEM. At least eight cells in each group were analyzed. ** $P < 0.01$, *** $P < 0.001$, one-way ANOVA. **(F, G)** EM analysis for subcellular localization of MARCKS and Rab10 in the corpus callosum regions from P0 rat brain. Arrows indicate immunogold particles (12 nm) for Rab10 signals associated with PPV-like vesicles, and arrowheads indicate immunogold particles (18 nm) for MARCKS on the PM **(F)**. Scale bar, 200 nm. The Rab10 and MARCKS localization is quantified **(G)**. At least 30 slices for each group were analyzed. **(H, I)** Quantification of the durations from docking to fusion for Rab10 vesicles in the rat fibroblasts transfected with the indicated plasmids. At least 10 cells in each group were analyzed. *** $P < 0.001$, Student's *t*-test. **(J)** Immuno-EM analysis for subcellular localization of Rab10-positive vesicles in fibroblasts transfected with vehicle or D3 plasmids. Yellow arrows point to immunogolds for Rab10. Red arrowhead indicates an omega-shaped Rab10-positive structure. Note that Rab10-positive vesicles are accumulated in the cell periphery in D3-transfected cells. Scale bars, 200 nm. **(K)** Quantification of the number of accumulated vesicles at a distance of 200 nm from PM, on or underneath 2 μ m length of PM. Data are presented as mean \pm SEM. At least eight cells in each group were analyzed. *** $P < 0.001$, Student's *t*-test.



in growing neurites [24]. We found that during the 30 min observation period, the disappearance of the red fluorescence in the longest neurite was largely dampened in neurons transfected with construct encoding siMARCKS, as compared to control neurons transfected with scrambled siRNA (Figure 5B and 5C). This result suggests that MARCKS is important for membrane insertion of PPVs in cultured cortical neurons.

Next, we directly measured vesicle docking and fusion in cortical neurons using TIRFM. As shown in Figure 5D, although epi-F signals of TD-Rab10 were detectable in all the neurites of a stage-3 neuron, the TIRF signals were present mainly in the distal region of axon and growth cone. By contrast, in siMARCKS neurons, the TIRF signals were markedly decreased, although epi-F signals remained in the soma and neuronal tips (Figure 5D and 5F). Notably, the intensity of TIRF signals in MARCKS D3-transfected neurons was increased and not limited to one neurite (Figure 5D and 5F). This result is consistent with the notion that MARCKS mediates docking of Rab10 vesicles to the PM via D3. Further, the role of MARCKS in membrane fusion of PPVs was measured in axonal growth cones by live imaging (Figure 5E and Supplementary information, Movie S5). As shown in Figure 5G, downregulation of MARCKS or overexpression of D3 caused a marked decrease in the membrane fusion of Rab10 vesicles in axonal growth cones.

The defects in membrane insertion and targeting of Rab10-PPVs might be caused by impairment in the biogenesis or the transport of Rab10 carriers, rather than membrane docking or fusion. To exclude these possibilities, we determined dynamics of TD-Rab10 vesicles in cultured cortical neurons transfected with siScramble or siMARCKS by live imaging. We found that both control and siMARCKS neurons had a number of dynamic Rab10 vesicles that exhibited random trajectory in the soma and some vesicles were transported into neurites

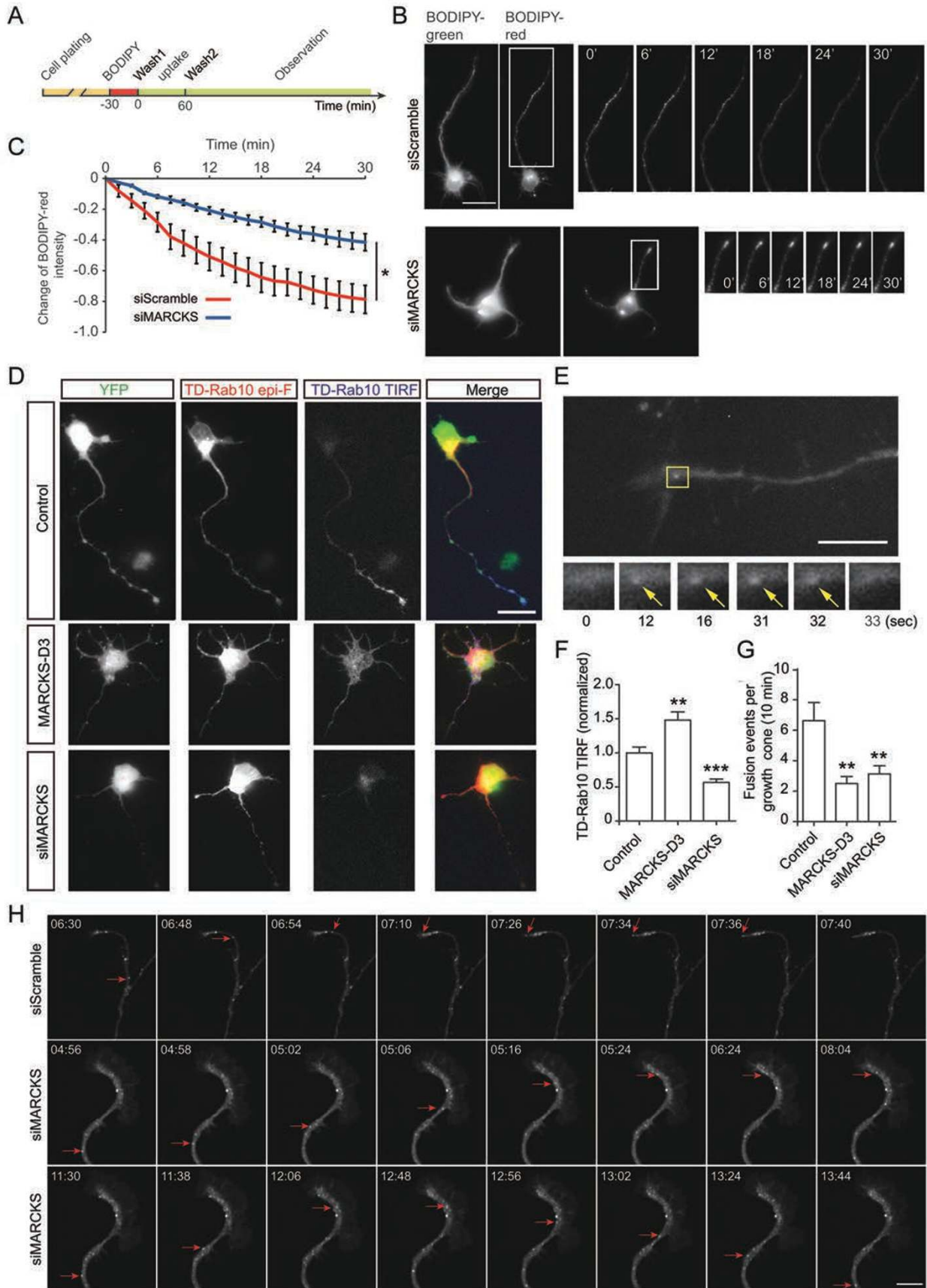
(Supplementary information, Movie S6). As shown in Figure 5H (top row) and Supplementary information, Movie S7, in control cells, the advance of anterograde vesicles was concurrent with or prior to growth cone extension, and, when arriving at the axonal tip, their fluorescence signals faded, reminiscent of membrane fusion. However, in siMARCKS cells, many Rab10 vesicles halted within growth cone and failed to fuse with axonal tips, and sometimes were transported back to the soma (Figure 5H, middle and bottom rows, and Supplementary information, Movie S7). We also quantified the transport of TD-Rab10 vesicles and found that MARCKS knock-down had no effect on the percentage or numbers of anterograde (from soma to neurite tips), retrograde (from tips to soma), or immobile vesicles, and the velocity of anterograde vesicles (Supplementary information, Figure S8A-S8F). These results suggest that MARCKS acts in the steps of vesicles docking/fusion, rather than formation or transport.

To determine spatial relationship between Rab10 and MARCKS in axonal growth cones, we co-transfected TD-Rab10 with S4N form of MARCKS-D3-YFP, a nonphosphorable form of D3 which was used to mark MARCKS sites on the PM, into cortical neurons. We found that, after arriving at the axonal growth cone, TD-Rab10 vesicles failed to fuse with the axonal membrane, and many of them were accumulated in MARCKS-D3 (S4N)-rich regions (Supplementary information, Movie S8 and Figure S8G). These results support again that D3 domain mediates membrane docking of Rab10 vesicles and the MARCKS-Rab10 interaction is also important for membrane fusion of Rab10-PPVs.

Relationships among actin dynamics, MARCKS, and Rab10 membrane fusion

It is believed that axon development requires coordination of actin dynamics, microtubule assembly, and

Figure 5 MARCKS is important for membrane insertion of Rab10 vesicles in primary neurons. **(A)** Schematic diagram illustrating BODIPY-ceramide labeling and observation procedure. **(B, C)** Cortical neurons transfected with vector encoding siMARCKS or scrambled sequences were labeled with BODIPY-ceramide at DIV2. The changes of BODIPY-red signals in the longest neurite were recorded using live-imaging fluorescence microscopy. At least five cells in each group were analyzed. $*P < 0.05$, paired *t*-test. Scale bar, 20 μm . **(D)** Cortical neurons were co-transfected with TD-Rab10 and pEYFP-N1 (control), MARCKS-D3-YFP, or pSUPER vector encoding siMARCKS. Epifluorescence (epi-F) and TIRF signals represent total and PM-associated TD-Rab10, respectively. Scale bar, 25 μm . **(E)** Live imaging of Rab10 TIRF signals in axonal growth cones of DIV2 cortical neurons transfected with TD-Rab10 and various plasmids. Shown is a representative image. Arrows point to a fusion event. Scale bar, 10 μm . **(F)** Quantification of the TIRF signals relative to epi-F signals. Average values from control group were normalized as 1.0. Data are presented as mean \pm SEM. 10 neurons in each group were analyzed. $**P < 0.01$, $***P < 0.001$, one-way ANOVA. **(G)** Quantification of the frequency of vesicle fusion in axonal growth cones. Data are presented as mean \pm SEM. 10 neurons in each group were analyzed. $**P < 0.01$, one-way ANOVA. **(H)** Snapshots of time-lapse images showing the movement of TD-Rab10 vesicles in axonal growth cone of DIV3 neurons transfected with siScramble or siMARCKS. Note the fading of transporting vesicles in axonal tip of control cell and persistence or retrograde transport in siMARCKS cells (red arrows). Scale bar, 10 μm . See also Supplementary information, Movies S6 and S7.



membrane trafficking [39]. Interestingly, treatment of cultured cortical neurons with actin de-polymerizing drug cytochalasin D at appropriate concentration (1 μ M) results in loss of actin in axonal growth cones, and surprisingly, promotes axon development [40]. In agreement with these results, we found that cytochalasin D (1 μ M) treatment of cultured cortical neurons exhibited similar effects, as reflected by decreased F-actin intensity in axons (Figure 6A and 6B), an increase in total axon length and the induction of multiple axons (Figure 6A and 6C). MARCKS has been shown to be an actin filament cross-linking protein [41, 42]. In line with this, we found that siMARCKS- or MARCKS D3-transfected neurons exhibited decreased actin in axonal growth cone, although to a much lesser extent than that caused by cytochalasin D (Figure 6A and 6B). However, in contrast to cytochalasin D, siMARCKS or D3 transfection inhibited axon development (Figure 6A and 6C). Thus it is unlikely that the defects in axon development caused by MARCKS manipulations were due to destabilization of actin networks. The relationship between actin dynamics and membrane insertion remains elusive. We have hypothesized that actin networks in cell cortex could be cytoskeleton barriers for vesicles tethering with the PM, and its spatial instability could facilitate vesicle docking and/or fusion. In support of this hypothesis, treatment with cytochalasin D (1 μ M, 1 h) increased membrane fusion of Rab10 vesicles (Figure 6D). Interestingly, this effect was not seen in siMARCKS cells (Figure 6D). Thus, MARCKS-mediated membrane targeting may coordinate with cytoskeleton dynamics in axon development. In line with this model, the effect of cytochalasin D in promoting axon development was abolished in siMARCKS- or D3-transfected cortical neurons (Figure 6C).

MARCKS regulates membrane targeting of axon growth-related receptors

Our previous study has shown that IGFR, the receptor for insulin-like growth factor, and TrkB, the receptor for brain-derived neurotrophic factor (BDNF), were present in Rab10-positive PPVs [24, 27]. Both IGFR and TrkB have been shown to be involved in axon development [43, 44]. In addition, vesicle-SNARE (soluble *N*-ethylmaleimide-sensitive fusion protein attachment protein receptor) proteins, such as VAMP4 [45] or VAMP7/TI-VAMP [34, 46-49], or target-SNARE proteins [50-52] are involved in neurite outgrowth. Exocyst complex appears to have an important role in polarized membrane insertion crucial for axon specification and elongation [53, 54]. Indeed, in axonal growth cones, vesicular Rab10 was largely colocalized with TrkB, IGFR, L1/NgCAM, TC10, VAMP4 or VAMP7, and to a much lesser extent

with VAMP2 or endosome marker EEA1 or endoplasmic reticulum (ER) markers GRP78/BiP and Calnexin (Supplementary information, Figure S9A-S9K). The relationship between MARCKS and these proteins in regulating behavior of Rab10 vesicles needs further investigation. The vesicular pools of cell adhesion molecule (L1/NgCAM) colocalized with Rab10 (Supplementary information, Figure S9C) may bridge membrane insertion and cell adhesion.

Given the role of MARCKS-Rab10 system in the docking and fusion of PPVs, we examined the membrane localization of IGFR and TrkB in cultured cortical neurons. We found that, whereas a fraction of IGFR or TrkB was localized on the membrane surface in control cells transfected with vehicle plasmid or scrambled siRNA (Figure 7A-7F), in D3-transfected or MARCKS-depleted cells, the membrane localization of both receptors was largely prevented (Figure 7A-7F). Thus, membrane targeting of Rab10-positive PPVs is required for the proper localization of neuronal surface proteins that are important for axon growth. In a most recent report, Rab10 has been shown to regulate ER dynamics [55]. We also found partial colocalization between Rab10 and ER marker Calnexin in axons with a much lesser extent (Supplementary information, Figure S9I). Thus, Rab10 has multifaceted roles in regulating behaviors of various cell organelles.

Discussion

Recently, we have shown that Rab10 is associated with PPVs [24], Myosin V controls biogenesis of post-Golgi Rab10 carriers [27], and JIP1 mediates anterograde transport of Rab10-PPVs during axon development [56]. How do Rab10 vesicles dock and fuse with the membrane at the destination sites? Here, we demonstrate a novel function of MARCKS in mediating membrane targeting of Rab10-positive PPVs and this process is required for axon development.

We found that Rab10 in its GTP-locked form binds to nonphosphorable form of MARCKS (Figure 1), which is an active form of MARCKS and localized on the PM to promote neurite initiation [16], spine elongation [15], growth cone adhesion and path finding [18], or dendritic branching [17]. This binding is direct and mediated by the MARCKS effector domain (Figure 1I-1O), which contains four serine phosphorylation sites [2]. Interestingly, both MARCKS and Rab10 were enriched in axonal tracts of the developing brain (Supplementary information, Figure S1). Given that Rab10 is required for axon development [24], we have investigated the role of MARCKS in axon development and found that

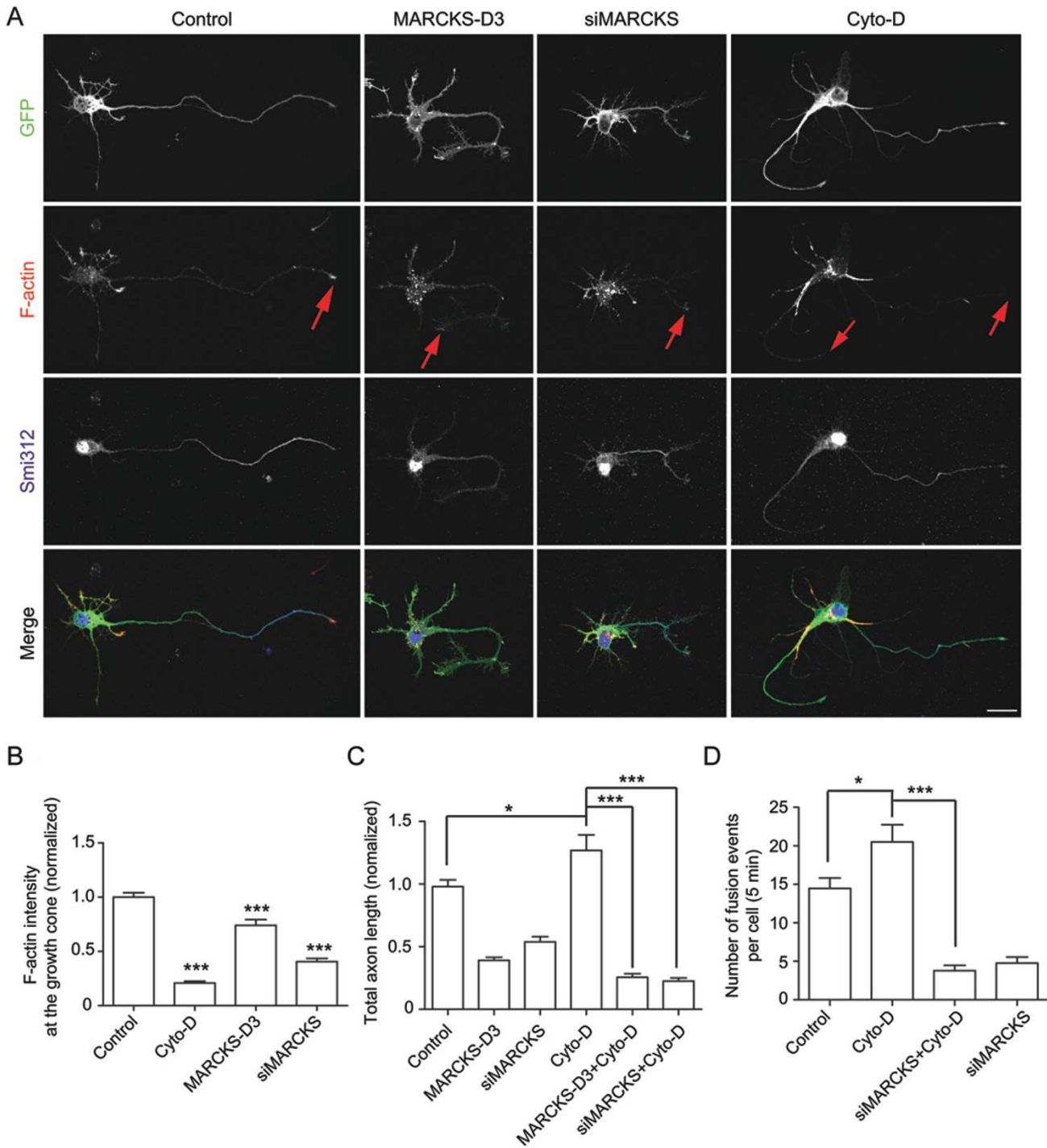


Figure 6 Coordination of actin dynamics and MARCKS in axon development and Rab10 vesicle fusion. **(A)** Neurons transfected with vehicle plasmid, siMARCKS or MARCKS-D3, together with GFP, were treated with DMSO or 1 μ M cytochalasin D at DIV2 for 24 h. At DIV3, cultures were stained with Smi312 and Alexa 647-labeled phalloidin. Scale bar, 20 μ m. Red arrows indicate phalloidin signals at neurite tips. **(B)** Quantification of normalized phalloidin intensity at the growth cone. Data are presented as mean \pm SEM of 20 neurons in each group. *** P < 0.001, Student's t -test. **(C)** Quantification of total axon length. Data are shown as mean \pm SEM. At least 180 neurons from two independent experiments were analyzed. * P < 0.05, *** P < 0.001, ANOVA with Student's t -test. **(D)** Quantification of average numbers of fusion events with complete cycles of docking and fusion during 5 min observation time in fibroblasts transfected with the indicated plasmids, without or with treatment with cytochalasin D (1 μ M, 1 h). Data are presented as mean \pm SEM of 9 cells in each group. * P < 0.05, *** P < 0.001, Student's t -test.

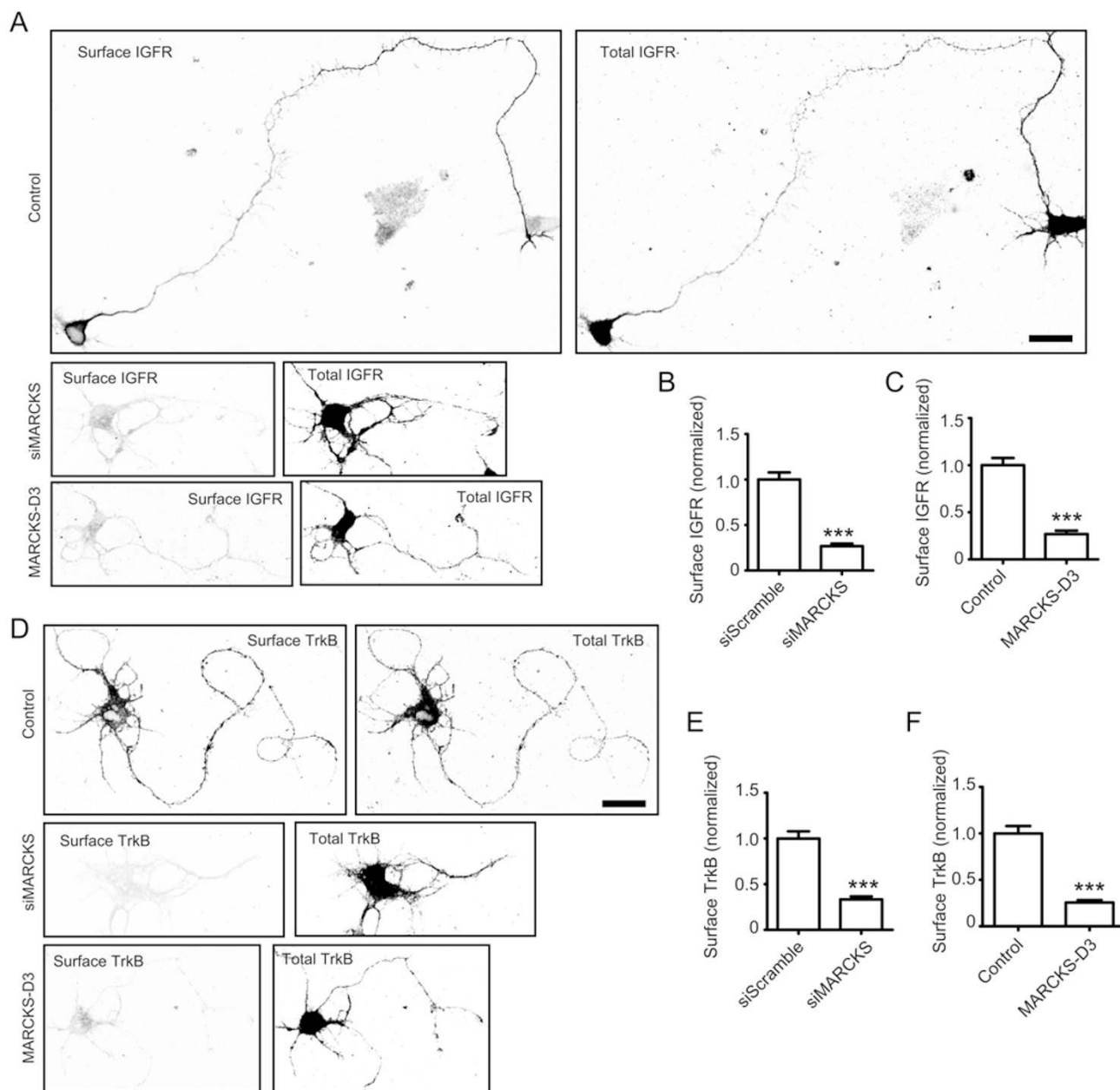


Figure 7 Role of MARCKS in surface expression of IGFR or TrkB. **(A, D)** Isolated cortical neurons were co-transfected with GFP-IGFR **(A)** or Flag-TrkB **(D)**, together with siMARCKS or D3 or vehicle plasmid. At DIV3, cells were live stained with antibody against FLAG or GFP to reveal surface levels of TrkB or IGFR, respectively. After surface labeling, cells were penetrated and stained for total IGFR or TrkB. Scale bar, 20 μ m. **(B, C, E, F)** Quantification of the surface levels of IGFR **(B, C)** or TrkB **(E, F)** in the indicated groups. Data are presented as mean \pm SEM with value from control group normalized as 1.0. *** $P < 0.01$ ($n = 10$ for each group), Student's t -test.

MARCKS is indeed necessary for Rab10's function in promoting axon growth (Figure 2E and 2F). Actually, MARCKS itself is important for axon development in isolated cortical neurons or neocortical neurons *in vivo* (Figure 2). We have also investigated the mechanism of MARCKS's action and concluded that MARCKS is a

component of docking and fusion machinery for Rab10-positive PPVs. The following lines of evidence support this conclusion: first, downregulation of MARCKS attenuated membrane insertion of PPVs labeled by BIOD-PY-ceramide in cultured cortical neurons (Figure 5A-5C); second, downregulating MARCKS or abrogating

its interaction with Rab10 caused a decrease in fusion frequency (Figure 4B and 4C) and interfered with vesicle fusion (Figure 4H, 4I and Supplementary information, Figure S4); third, EM analysis showed a close apposition between Rab10-positive vesicles and MARCKS-labeled PM sites (Figure 4F and 4G); and finally, disrupting the interaction between MARCKS and Rab10 caused accumulation of PPVs at the cell periphery (Figure 4J and 4K) or axonal growth cones (Supplementary information, Movie S8 and Figure S8G) without fusion. Thus, we propose that MARCKS residing on the PM acts as a component of docking/fusion machinery for Rab10-positive vesicles (Figure 8). Our data do not preclude the involvement of SNARE or exocyst complexes in regulating docking or fusion of Rab10 vesicles. The relationship between MARCKS and these proteins needs further investigation. Given that MARCKS association with the PM is transient and is regulated by phosphorylation, we predict that MARCKS may recruit Rab10 vesicles to the fusion “hotspots”, which contain SNARE or other fusion machinery proteins. The presence of MARCKS in this complex determine selective docking/fusion of Rab10 vesicles.

It seems that MARCKS functions in several neural developmental stages. For example, MARCKS deficiency leads to ectopic placement and proliferation of radial progenitors, and consequently defective neuronal lamination [19]. To circumvent this complexity, we did electroporation at E16.5, when layer II/III neurons are born,

and observed corpus callosum axon projections on P2. We found that downregulation of MARCKS or expression of D3 markedly affected callosal axon projections, without apparent effect on cell positioning at this observation period (Figures 2G and 3E). The conclusion that MARCKS is essential for axon development has also been confirmed in isolated cultured cortical neurons. We have shown recently that Myosin V controls fission of Rab10 carriers from the TGN [27]. This study has identified MARCKS as a component of machinery responsible for the docking/fusion of Rab10 vesicles. It is interesting to understand how Rab10 switches binding partners in these consecutive stages.

Besides Rab10, other Rabs, such as Rab8 and Rab21, have been implicated in membrane insertion as well as axon development [23, 34]. Different Rabs may cooperate in controlling exocytotic process at various steps. For example, Rab8 has been proposed to mediate docking and fusion of Rab6-positive vesicles through interaction with a protein complex associated with the PM [57]. The relationship between these Rabs and the MARCKS-Rab10 system demonstrated here will be a topic of great interest.

Materials and Methods

Reagents and antibodies

Neurobasal and B27 were from Invitrogen. OA and DES were from Calbiochem. Cytochalasin D was from Sigma Aldrich. Staurosporine was from Cell Signaling. Hoechst 33342 and DAPI were

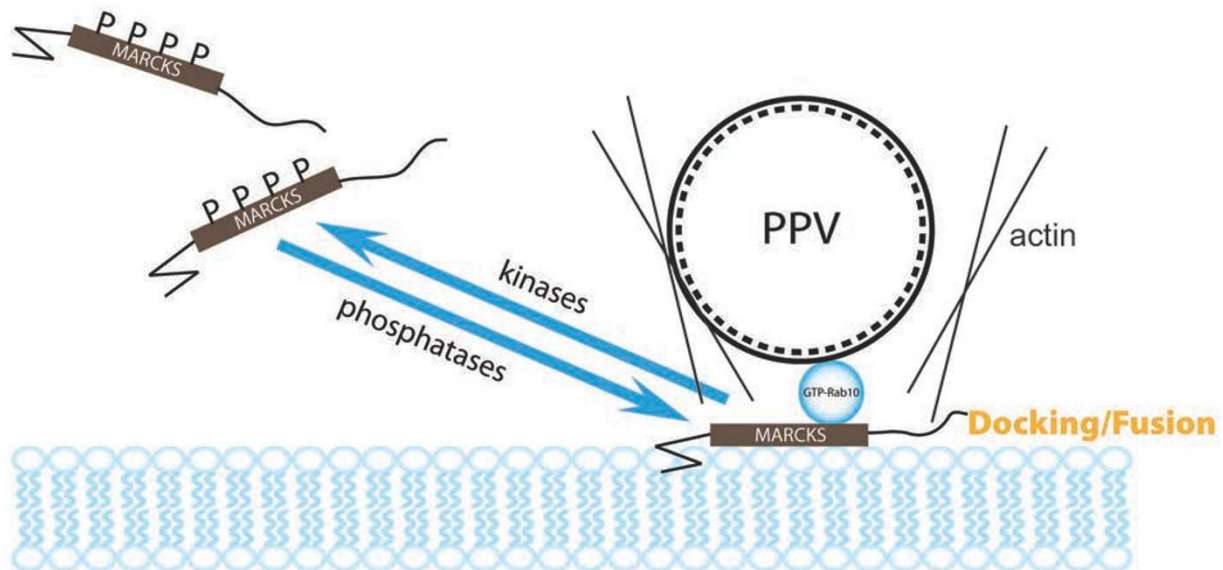


Figure 8 Proposed model for membrane targeting of Rab10 vesicles. Membrane-associated MARCKS interacts with GTP-bound form of Rab10, in a manner dependent on phosphorylation status of MARCKS effector domain, and mediates membrane targeting of Rab10-positive PPVs. This process may be coordinated with cytoskeleton dynamics.

from Beyotime. Beads used for affinity purification were from GE (Glutathione-sepharose), Roche (protein A or protein G agarose), or Qiagen (Ni-NTA). Antibodies used for immunostaining or immunoblotting were from Protein Tech Group (Rab10, GST), Santa Cruz (Myc, GFP, TC10, JIP1, MARCKS, p-MARCKS (Ser170), p-MARCKS (Ser152/156)), Sigma (HA, Actin), Abcam (His, EEA1, L1, VAMP2, VAMP4, VAMP7), Enzo (Calnexin, PIP2), Invitrogen (GFP), Aves Labs (GFP), Abmart (Rab10, GFP), Covance (Smi312, Tuj1), KangChen (GAPDH), BD (Rab8), Upstate (Rab11), Millipore (TrkB), or Cell signaling (IGFR- β). Alexa 488-, Alexa 555-, or Alexa 647-conjugated secondary antibodies and Alexa 647-phalloidin were from Invitrogen or Jackson ImmunoResearch. HRP-conjugated secondary antibodies were from Millipore. BODIPY[®] FL C5-ceramide was from Invitrogen. Plasma membrane protein extraction kit was from Biovision.

Constructs

The WT MARCKS and mutants (G2A, S4N, S4D, DBL) were introduced in previous studies [32, 33]. Different domains of MARCKS (D1, aa 1-36; D2, aa 10-150; and D3, aa 138-184) were subcloned into pEYFP-N1 with EYFP epitopes at the C-terminus. D3 was also inserted into pCS2 + MT in frame with 6 \times Myc epitopes at the C-terminus, or into pGEX-2T to produce GST-fusion proteins. TD-Rab10 was generated by inserting tdTomato sequence into pKH3-Rab10 at the *Hind*III site. TD-Rab11 was constructed by replacing Rab10 sequence with Rab11 sequence between the *Bam*HI and *Eco*RI sites of TD-Rab10 plasmid. Other Rab10 constructs were introduced in our previous study [24].

siRNAs

The siRNA sequence was designed against nucleotides 2 036-2 054 of rat MARCKS with the following sequences: 5'-CTGTAC-CAGTCAGTAATTA-3' (sense) and 5'-TAATTAAGTACTGG-TACAG-3' (antisense). The sequences of scrambled siRNA were: 5'-GCGCGCTATGTAGGATTCG-3' (sense) and 5'-CGAATCCTA-CATAGCGCGC-3' (antisense). All double-stranded oligonucleotides were synthesized by GenePharma (Shanghai, China) and subcloned into pSUPER vector.

Biochemical characterization, BODIPY-ceramide labeling and fluorescence observation

For co-immunoprecipitation assay of endogenous proteins, P0 rat brains were homogenized in lysis buffer containing 50 mM Tris-HCl, pH 7.4, 150 mM NaCl, 1% Nonidet P-40, and protease inhibitors. Lysates were clarified by centrifugation (15 000 \times g for 30 min at 4 $^{\circ}$ C). The soluble supernatants were incubated with protein G agarose beads conjugated with Rab10/MARCKS antibodies or normal control IgG overnight at 4 $^{\circ}$ C. Beads were washed three times in lysis buffer and bound proteins were eluted by boiling in 2 \times SDS loading buffer, followed by immunoblotting with the indicated antibodies. The guanine nucleotide selective binding assay was performed according to a previous report [58]. Briefly, GST-Rab10 (5 μ g) immobilized on glutathione-sepharose beads or purified His6-Rab10 (2 μ g) was incubated with 30 μ M GTP γ S or GDP at 30 $^{\circ}$ C for 1 h in a reaction buffer (25 mM Tris-HCl, pH 7.5, 10 mM EDTA, 1 mM DTT, and 5 mM MgCl₂) before incubation with His6-D3 (2 μ g) or GST-MARCKS (5 μ g) at 30 $^{\circ}$ C for 1 h. BODIPY-ceramide labeling, fluorescence observation and signal quantification were performed as described in our previous

study [24].

Affinity purification and mass spectrometry

Brain homogenates from P0 SD rats in the lysis buffer (50 mM Tris, pH 7.5, 150 mM NaCl, 1% Nonidet P-40) were centrifuged twice at 16 000 \times g for 30 min at 4 $^{\circ}$ C to clear tissue debris. Supernatants (1 mg protein/ml) were first incubated with empty glutathione agarose beads to reduce nonspecific binding (2 h, 4 $^{\circ}$ C), followed by incubation with beads immobilized with GST-Rab10 (50 μ g) in the presence of 30 μ M GTP γ S and 5 mM Mg²⁺ for 2 h at 30 $^{\circ}$ C. Bound proteins were eluted by reduced glutathione (20 mM in 50 mM Tris, pH 8.0) for 30 min at room temperature (RT), concentrated and incubated with trypsin (20 ng/ml) at 37 $^{\circ}$ C for 16 h. Peptides from affinity-purified proteins were separated using reverse phase high performance liquid chromatography (RP-HPLC) on a self-packed column and analyzed with an LTQ-Orbitrap instrument (Thermo Fisher Scientific), which was operated in data-dependent mode with a resolution of R = 60 000 at m/z 400. The obtained MS/MS spectra were searched using Maxquant software against the Rat International Protein Index (IPI) database (version 3.68).

Cell culture, transfection, and imaging

Rat fibroblasts were isolated from E18.5 fetal rat skin and cultured in DMEM supplemented with 10% fetal bovine serum (FBS) in a 37 $^{\circ}$ C incubator with 5% CO₂. Rat cortical neurons were prepared as described previously [59]. Dissociated cells were transfected by electroporation using the Amaxa Nucleofector device. Neurons were plated onto coverslips coated with poly-D-lysine. After culturing for 24 h, media was changed to neuronal culture media (Neurobasal media containing 1% glutamate and 2% B27). HEK293 cells were cultured and transfected as described [24].

For the analysis of subcellular localization, cells were fixed and stained with the indicated antibodies, and fluorescence images were taken using a 60 \times Plan Apo objective (NA 1.4 oil) on the NIKON A1R inverted confocal microscope. For axon length analysis, neurons were fixed and stained 72 h after plating with Smi312 and Tuj1 antibodies. The fixed and stained cultures were examined by the NeuroLucida system (Nikon).

For live imaging of membrane fusion of Rab10 vesicles, cells kept in a stage top incubator (model INUG2E-ZILCS, Tokai Hit) at 37 $^{\circ}$ C were observed with an inverted motorized microscope (Nikon TE2000-U) through a 100 \times 1.49 oil Apo TIRF objective lens. Images were captured using a CCD camera and analyzed with Image J software. Time-lapse images were acquired at high rates (3 frames/sec) to monitor vesicle docking and fusion in fibroblast and at slow rates (1 frame/sec) in neurons.

To monitor the transport of TD-Rab10 vesicles, cortical neurons were transfected with TD-Rab10 together with siScramble or siMARCKS before plating. At DIV3, cells were kept in an incubator at 37 $^{\circ}$ C with 5% CO₂ during imaging process. Time-lapse images were acquired at intervals of 2 s for 15 min using NIKON A1R inverted confocal microscope with Apo TIRF 60 \times object lens. Kymographs were generated with Image J software.

FRET assay

Interaction between Rab10 and MARCKS *in situ* was determined by FRET analysis using acceptor photobleaching protocol. Fluorescence signals were collected with a TCS SP5 LSM confo-

cal microscope (Leica) using laser excitation at 488 nm (eGFP) and 554 nm (tdTomato), emission windows of 505–530 nm, and a 560–615-nm-long pass filter. Preceding the emission filters in the light path was a NFT 545-nm dichroic mirror that split the eGFP and tdTomato signals to distinct photomultiplier tubes. All fluorescence data were collected with a 63× 1.3 numerical aperture objective (Leica). Photobleaching in selective regions (either a whole cell or region of interest (ROI) of a cell) was irradiated with the 554-nm laser line (100% intensity, 60 iterations, using a 488-nm/543-nm dual dichroic mirror) for 30–50 times to bleach tdTomato to obtain < 40% bleaching rate. Images were acquired before and after photobleaching. FRET efficiency (E) between eGFP (donor) and tdTomato (acceptor) was auto-quantified by Lecia AF FRET system using the following Equation ($E = (D_{post} - D_{pre})/D_{post}$) in which D_{pre} and D_{post} are eGFP emission with 488 nm excitation in the photobleached region before and after photobleaching with 554 nm excitation, respectively.

Surface labeling of membrane proteins

Isolated cortical neurons were co-transfected with Flag-TrkB or GFP-IGFR, together with siMARCKS or D3 or vehicle plasmid. At DIV3, cells grown on coverslips were incubated at 37 °C with mouse anti-Flag or chicken anti-GFP antibody (1:100 in DMEM containing 1% BSA and 5% FBS) for 60 min. After 4× washes with DMEM, cells were fixed with 4% paraformaldehyde (PFA) at RT for 30 min, washed with PBS for 3 times, permeabilized with 0.1% Triton X-100 for 10 min, blocked with 1% BSA in PBS, and incubated with primary antibody (rabbit anti-TrkB antibody or rabbit anti-IGFR antibody) at 4 °C overnight. After 3× washes with PBS, samples were incubated with secondary antibodies (Alexa 647-conjugated donkey anti-rabbit IgG, Alexa 555-conjugated donkey anti-chicken IgY or Alexa 555-conjugated donkey anti-mouse IgG) for 2 h. Microscopic images were taken using a 60× Plan Apo objective (NA 1.4 oil) on the NIKON A1R inverted confocal microscope.

Electron microscopy and immunoelectron microscopy

Cells or brain sections from corpus callosum regions of P0 rats were fixed for 1 h with 2.5% glutaraldehyde in 0.1 M PBS, pH 7.4, followed by post-fixation with 1% osmium tetroxide for 30 min, 3× washes with 0.1 M PBS, dehydration in ascending ethanol series, and finally embedded in araldite over 2 days. Thin sections were stained with methanolic uranyl acetate and lead citrate for morphological examination. Sections were then observed with a Joel JEM-1230 TEM.

Cells or brain samples from corpus callosum regions of P0 rats were fixed by 4% PFA, 0.1% picric acid and 0.05% glutaraldehyde in 0.1 M PBS for 2 h at 4 °C, then cut into 200-µm slices and incubated with 1% osmic oxide for 30 min, dehydrated and embedded in Epon 812. Polymerization was carried out at 37 °C for 12 h, 45 °C for 12 h and 60 °C for 24 h. Ultra-thin sections were cut and collected on nickel grids (200 mesh), followed by staining with primary antibodies against MARCKS (1:100; Santa Cruz) and Rab10 (1:50; Protein Tech Group) at 4 °C for 48 h, extensive washes with PBS (10× 10 min), and then incubation with secondary antibodies conjugated with 18-nm and 12-nm gold particles (1:100, Jackson ImmunoResearch) at RT for 2 h. After extensive washes with PBS (10× 10 min), sections were incubated with methanolic uranyl acetate and lead citrate, and then observed with a Joel JEM-1230 TEM.

In utero electroporation

As described previously [60], embryonic rat brains were subjected to electroporation, following the injection of mixtures of plasmid DNA in Fast Green (Amresco). Briefly, DNA mixtures containing 9 µg of a plasmid encoding siRNA against MARCKS or a scrambled sequence, and 3 µg pCAG-EYFP plasmid, were injected into the lateral ventricle of the rat brains at E16.5, which were then subjected to electroporation consisting of five square wave pulses (55 V, 100 ms) with an interval of 1 s (ECM830; BTX). Seven days post electroporation, coronal cryostat sections of P2 rat cortex were immediately processed for immunostaining with a free-floating protocol. Briefly, brain slices, after treatment with 0.3% Triton X-100 and 5% goat serum in PBS for 1 h, were incubated with primary antibodies for 24 h at 4 °C, followed by 3× washes with PBS, and incubation with Alexa fluorescence-conjugated secondary antibodies. All the animal experiments were performed in accordance with institutional guidelines and regulations.

Acknowledgments

This work was supported by the National Natural Science Foundation of China (31330032, 31321091, and 61327902 to ZG L and 81171190 to XH X) and the National Key Basic Research Program of China (2014CB910203). We thank Dr Q Hu of ION Imaging Facility with microscope analysis and Dr Y Kong with EM analysis. XH X was supported by SA-SIBS Scholarship Program, Shanghai Postdoctoral Scientific Program, China Postdoctoral Science Foundation funded Project, and KC Wong Education Foundation.

References

- 1 Wu WC, Walaas SI, Nairn AC, Greengard P. Calcium/phospholipid regulates phosphorylation of a Mr “87k” substrate protein in brain synaptosomes. *Proc Natl Acad Sci USA* 1982; **79**:5249–5253.
- 2 Stumpo DJ, Graff JM, Albert KA, Greengard P, Blackshear PJ. Molecular cloning, characterization, and expression of a cDNA encoding the “80- to 87-kDa” myristoylated alanine-rich C kinase substrate: a major cellular substrate for protein kinase C. *Proc Natl Acad Sci USA* 1989; **86**:4012–4016.
- 3 Rosen A, Keenan KF, Thelen M, Nairn AC, Aderem A. Activation of protein kinase C results in the displacement of its myristoylated, alanine-rich substrate from punctate structures in macrophage filopodia. *J Exp Med* 1990; **172**:1211–1215.
- 4 George DJ, Blackshear PJ. Membrane association of the myristoylated alanine-rich C kinase substrate (MARCKS) protein appears to involve myristate-dependent binding in the absence of a myristoyl protein receptor. *J Biol Chem* 1992; **267**:24879–24885.
- 5 Swierczynski SL, Blackshear PJ. Membrane association of the myristoylated alanine-rich C kinase substrate (MARCKS) protein. Mutational analysis provides evidence for complex interactions. *J Biol Chem* 1995; **270**:13436–13445.
- 6 Allen LA, Aderem A. Protein kinase C regulates MARCKS cycling between the plasma membrane and lysosomes in fibroblasts. *EMBO J* 1995; **14**:1109–1121.
- 7 Hartwig JH, Thelen M, Rosen A, Janmey PA, Nairn AC,

- Aderem A. MARCKS is an actin filament crosslinking protein regulated by protein kinase C and calcium-calmodulin. *Nature* 1992; **356**:618-622.
- 8 Laux T, Fukami K, Thelen M, Golub T, Frey D, Caroni P. GAP43, MARCKS, and CAP23 modulate PI(4,5)P(2) at plasmalemmal rafts, and regulate cell cortex actin dynamics through a common mechanism. *J Cell Biol* 2000; **149**:1455-1472.
- 9 Myat MM, Anderson S, Allen LA, Aderem A. MARCKS regulates membrane ruffling and cell spreading. *Curr Biol* 1997; **7**:611-614.
- 10 Walaas SI, Nairn AC, Greengard P. Regional distribution of calcium- and cyclic adenosine 3':5'-monophosphate-regulated protein phosphorylation systems in mammalian brain. II. Soluble systems. *J Neurosci* 1983; **3**:302-311.
- 11 Albert KA, Walaas SI, Wang JK, Greengard P. Widespread occurrence of "87 kDa," a major specific substrate for protein kinase C. *Proc Natl Acad Sci USA* 1986; **83**:2822-2826.
- 12 Ouimet CC, Wang JK, Walaas SI, Albert KA, Greengard P. Localization of the MARCKS (87 kDa) protein, a major specific substrate for protein kinase C, in rat brain. *J Neurosci* 1990; **10**:1683-1698.
- 13 Blackshear PJ, Wen L, Glynn BP, Witters LA. Protein kinase C-stimulated phosphorylation in vitro of a Mr 80,000 protein phosphorylated in response to phorbol esters and growth factors in intact fibroblasts. Distinction from protein kinase C and prominence in brain. *J Biol Chem* 1986; **261**:1459-1469.
- 14 Stumpo DJ, Bock CB, Tuttle JS, Blackshear PJ. MARCKS deficiency in mice leads to abnormal brain development and perinatal death. *Proc Natl Acad Sci USA* 1995; **92**:944-948.
- 15 Calabrese B, Halpain S. Essential role for the PKC target MARCKS in maintaining dendritic spine morphology. *Neuron* 2005; **48**:77-90.
- 16 Shiraishi M, Tanabe A, Saito N, Sasaki Y. Unphosphorylated MARCKS is involved in neurite initiation induced by insulin-like growth factor-I in SH-SY5Y cells. *J Cell Physiol* 2006; **209**:1029-1038.
- 17 Li H, Chen G, Zhou B, Duan S. Actin filament assembly by myristoylated alanine-rich C kinase substrate-phosphatidylinositol-4,5-diphosphate signaling is critical for dendrite branching. *Mol Biol Cell* 2008; **19**:4804-4813.
- 18 Gatlin JC, Estrada-Bernal A, Sanford SD, Pfenninger KH. Myristoylated, alanine-rich C-kinase substrate phosphorylation regulates growth cone adhesion and pathfinding. *Mol Biol Cell* 2006; **17**:5115-5130.
- 19 Weimer JM, Yokota Y, Stanco A, Stumpo DJ, Blackshear PJ, Anton ES. MARCKS modulates radial progenitor placement, proliferation and organization in the developing cerebral cortex. *Development* 2009; **136**:2965-2975.
- 20 Bjorkblom B, Padzik A, Mohammad H, *et al.* c-Jun N-terminal kinase phosphorylation of MARCKSL1 determines actin stability and migration in neurons and in cancer cells. *Mol Cell Biol* 2012; **32**:3513-3526.
- 21 Stenmark H. Rab GTPases as coordinators of vesicle traffic. *Nat Rev Mol Cell Biol* 2009; **10**:513-525.
- 22 Grosshans BL, Andreeva A, Gangar A, *et al.* The yeast Igl family member Sro7p is an effector of the secretory Rab GTPase Sec4p. *J Cell Biol* 2006; **172**:55-66.
- 23 Huber LA, Dupree P, Dotti CG. Use of antisense oligonucleotides to study Rab function *in vivo*. *Methods Enzymol* 1995; **257**:302-312.
- 24 Wang T, Liu Y, Xu XH, *et al.* Lgl1 activation of Rab10 promotes axonal membrane trafficking underlying neuronal polarization. *Dev Cell* 2011; **21**:431-444.
- 25 Sano H, Egeuz L, Teruel MN, *et al.* Rab10, a target of the AS160 Rab GAP, is required for insulin-stimulated translocation of GLUT4 to the adipocyte plasma membrane. *Cell Metab* 2007; **5**:293-303.
- 26 Roland JT, Lapierre LA, Goldenring JR. Alternative splicing in class V myosins determines association with Rab10. *J Biol Chem* 2009; **284**:1213-1223.
- 27 Liu Y, Xu XH, Chen Q, *et al.* Myosin Vb controls biogenesis of post-Golgi Rab10 carriers during axon development. *Nat Commun* 2013; **4**:2005.
- 28 Graff JM, Rajan RR, Randall RR, Nairn AC, Blackshear PJ. Protein kinase C substrate and inhibitor characteristics of peptides derived from the myristoylated alanine-rich C kinase substrate (MARCKS) protein phosphorylation site domain. *J Biol Chem* 1991; **266**:14390-14398.
- 29 Arbuzova A, Schmitz AA, Vergeres G. Cross-talk unfolded: MARCKS proteins. *Biochem J* 2002; **362**:1-12.
- 30 Clarke PR, Siddhanti SR, Cohen P, Blackshear PJ. Okadaic acid-sensitive protein phosphatases dephosphorylate MARCKS, a major protein kinase C substrate. *FEBS Lett* 1993; **336**:37-42.
- 31 Dobrowsky RT, Kamibayashi C, Mumby MC, Hannun YA. Ceramide activates heterotrimeric protein phosphatase 2A. *J Biol Chem* 1993; **268**:15523-15530.
- 32 Swierczynski SL, Siddhanti SR, Tuttle JS, Blackshear PJ. Nonmyristoylated MARCKS complements some but not all of the developmental defects associated with MARCKS deficiency in mice. *Dev Biol* 1996; **179**:135-147.
- 33 Spizz G, Blackshear PJ. Overexpression of the myristoylated alanine-rich C-kinase substrate inhibits cell adhesion to extracellular matrix components. *J Biol Chem* 2001; **276**:32264-32273.
- 34 Burgo A, Proux-Gillardeaux V, Sotirakis E, *et al.* A molecular network for the transport of the TI-VAMP/VAMP7 vesicles from cell center to periphery. *Dev Cell* 2012; **23**:166-180.
- 35 Pfenninger KH. Plasma membrane expansion: a neuron's Herculean task. *Nat Rev Neurosci* 2009; **10**:251-261.
- 36 Dajas-Bailador F, Jones EV, Whitmarsh AJ. The JIP1 scaffold protein regulates axonal development in cortical neurons. *Curr Biol* 2008; **18**:221-226.
- 37 Shirane M, Nakayama KI. Protrudin induces neurite formation by directional membrane trafficking. *Science* 2006; **314**:818-821.
- 38 Pagano RE, Martin OC, Kang HC, Haugland RP. A novel fluorescent ceramide analogue for studying membrane traffic in animal cells: accumulation at the Golgi apparatus results in altered spectral properties of the sphingolipid precursor. *J Cell Biol* 1991; **113**:1267-1279.
- 39 Arimura N, Kaibuchi K. Neuronal polarity: from extracellular signals to intracellular mechanisms. *Nat Rev Neurosci* 2007; **8**:194-205.
- 40 Bradke F, Dotti CG. The role of local actin instability in axon formation. *Science* 1999; **283**:1931-1934.
- 41 Hartwig JH, Thelen M, Rosen A, Janmey PA, Nairn AC,

- Aderem A. Marcks is an actin filament cross-linking protein regulated by protein-kinase-c and calcium calmodulin. *Nature* 1992; **356**:618-622.
- 42 Laux T, Fukami K, Thelen M, Golub T, Frey D, Caroni P. GAP43, MARCKS, and CAP23 modulate PI(4,5)P-2 at plasmalemmal rafts, and regulate cell cortex actin dynamics through a common mechanism. *J Cell Biol* 2000; **149**:1455-1471.
- 43 Sosa L, Dupraz S, Laurino L, *et al.* IGF-1 receptor is essential for the establishment of hippocampal neuronal polarity. *Nat Neurosci* 2006; **9**:993-995.
- 44 Shelly M, Cancedda L, Heilshorn S, Sumbre G, Poo MM. LKB1/STRAD promotes axon initiation during neuronal polarization. *Cell* 2007; **129**:565-577.
- 45 Cocucci E, Racchetti G, Rupnik M, Meldolesi J. The regulated exocytosis of enlargeosomes is mediated by a SNARE machinery that includes VAMP4. *J Cell Sci* 2008; **121**:2983-2991.
- 46 Coco S, Raposo G, Martinez S, *et al.* Subcellular localization of tetanus neurotoxin-insensitive vesicle-associated membrane protein (VAMP)/VAMP7 in neuronal cells: evidence for a novel membrane compartment. *J Neurosci* 1999; **19**:9803-9812.
- 47 Martinez-Arca S, Coco S, Mainguy G, *et al.* A common exocytotic mechanism mediates axonal and dendritic outgrowth. *J Neurosci* 2001; **21**:3830-3838.
- 48 Martinez-Arca S, Alberts P, Zahraoui A, Louvard D, Galli T. Role of tetanus neurotoxin insensitive vesicle-associated membrane protein (TI-VAMP) in vesicular transport mediating neurite outgrowth. *J Cell Biol* 2000; **149**:889-900.
- 49 Gupton SL, Gertler FB. Integrin signaling switches the cytoskeletal and exocytic machinery that drives neuritogenesis. *Dev Cell* 2010; **18**:725-736.
- 50 Igarashi M, Kozaki S, Terakawa S, Kawano S, Ide C, Komiya Y. Growth cone collapse and inhibition of neurite growth by *Botulinum* neurotoxin C1: a t-SNARE is involved in axonal growth. *J Cell Biol* 1996; **134**:205-215.
- 51 Osen-Sand A, Staple JK, Naldi E, *et al.* Common and distinct fusion proteins in axonal growth and transmitter release. *J Comp Neurol* 1996; **367**:222-234.
- 52 Darios F, Davletov B. Omega-3 and omega-6 fatty acids stimulate cell membrane expansion by acting on syntaxin 3. *Nature* 2006; **440**:813-817.
- 53 Dupraz S, Grassi D, Bernis ME, *et al.* The TC10-Exo70 complex is essential for membrane expansion and axonal specification in developing neurons. *J Neurosci* 2009; **29**:13292-13301.
- 54 Lalli G. RaLa and the exocyst complex influence neuronal polarity through PAR-3 and aPKC. *J Cell Sci* 2009; **122**:1499-1506.
- 55 English AR, Voeltz GK. Rab10 GTPase regulates ER dynamics and morphology. *Nat Cell Biol* 2013; **15**:169-178.
- 56 Deng CY, Lei WL, Xu XH, Ju XC, Liu Y, Luo ZG. JIP1 mediates anterograde transport of Rab10 cargos during neuronal polarization. *J Neurosci* 2014; **34**:1710-1723.
- 57 Grigoriev I, Yu KL, Martinez-Sanchez E, *et al.* Rab6, Rab8, and MICAL3 cooperate in controlling docking and fusion of exocytotic carriers. *Curr Biol* 2011; **21**:967-974.
- 58 Arimura N, Kimura T, Nakamura S, *et al.* Anterograde transport of TrkB in axons is mediated by direct interaction with Slp1 and Rab27. *Dev Cell* 2009; **16**:675-686.
- 59 Xu X, He C, Zhang Z, Chen Y. MKLP1 requires specific domains for its dendritic targeting. *J Cell Sci* 2006; **119**:452-458.
- 60 Saito T, Nakatsuji N. Efficient gene transfer into the embryonic mouse brain using *in vivo* electroporation. *Dev Biol* 2001; **240**:237-246.

(Supplementary information is linked to the online version of the paper on the *Cell Research* website.)